Research Report

98-50

Flux Tracking Methods for Direct Field Orientation

M.D. Manjrekar, T.A. Lipo, S.-G. Chang*, K.-S. Kim*

Wisconsin Power Electronic
Research Center
University of Wisconsin-Madison
Madison WI 53706-1691

*LGIS R&D Center
LG Industrial Systems Co., Ltd.
Seoul, Korea

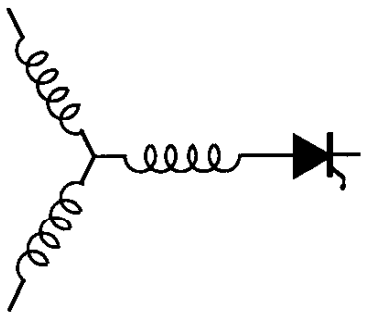

Wisconsin
Electric
Machines &
Power
Electronics
Consortium

University of Wisconsin-Madison
College of Engineering
Wisconsin Power Electronics Research Center
2559D Engineering Hall
1415 Engineering Drive
Madison WI 53706-1691

Flux Tracking Methods for Direct Field Orientation

Madhav D. Manjrekar Thomas A. Lipo
Department of Electrical and Computer Engineering,
University of Wisconsin – Madison,
Madison, WI, 53706, USA.

Seo-Geon Chang Kyung-Seo Kim
LGIS R&D Center,
LG Industrial Systems Co., Ltd.,
Seoul, Korea.

Abstract - **Numerous techniques have been reported in the literature to accomplish the task of locating the rotor flux axis for the purpose of direct field orientation. This paper first summarizes the existing sensorless techniques using high frequency test signal injection to determine the flux spatial location in an induction machine. A novel approach employing balanced and unbalanced excitation is then investigated to track the flux. It is first demonstrated that the rotating flux vector in the machine causes saturation-induced saliency in the phases under normal operating conditions. By employing high frequency test signals, this saliency is monitored which is then used to track the flux in the machine under test. The feasibility of the proposed approach is verified with experimental results.**

I. Introduction

Accurate control of torque production is possible in an induction machine drive when the flux and torque producing components in the stator current are controlled independently [1], [2]. This type of control is referred to as 'Vector Control' because it includes the precise adjustment of both amplitude and phase of the ac excitation. Vector control of currents and voltages ultimately results in manipulation of the spatial orientation of the electromagnetic fields in the machine. This has led to the term 'Field Orientation'. Normally, torque control by direct field orientation refers to the process of locating the spatial position of rotor flux in the machine and the consequent control of the quadrature component of stator magnetomotive force (mmf), produced by stator current, with respect to this flux.

Numerous techniques have been reported in the literature to accomplish the task of locating the rotor flux axis [3]-[10]. This paper investigates a novel method of high frequency test signal injection to locate the flux in an induction machine. It is first demonstrated that the rotating flux vector in the machine causes saturation-induced saliency in the phases under normal operating conditions. By employing high frequency test signals, this saliency is monitored which is then used to track the flux in the machine. These flux tracking methods are employed to accomplish direct field orientation for torque control applications.

The following sections of this paper present a review of vector control and high frequency test signal injection techniques used to locate the rotor flux angle which have been previously reported in the literature. A new flux tracking method based on phase impedance variation is then introduced in Section IV. Techniques employing balanced and unbalanced excitation to detect the phase impedance variation and their practical implementation are described in Section V. Experimental results verifying the efficacy of the proposed approach are given in Section VI. A summary of these results and a discussion of the advantages and limitations of the proposed approach is presented in the concluding section.

II. D-Q Representation Of Vector Control

In terms of the machine variables in the rotor flux synchronous frame of reference [2], the electromagnetic torque is given by

$$T_e = \frac{3}{2}\frac{P}{2}\frac{L_m}{L_r}\lambda^e_{dr} i^e_{qs} \qquad (1)$$

The symbols for torque, inductance, current and flux follow the convention used in [2]. If the d–axis is considered as the rotor flux axis, the rotor flux is given by the following differential equation

$$(r_r + L_r p)\lambda^e_{dr} = r_r L_m i^e_{ds} \qquad (2)$$

where p is the differential operator. Thus the equation for torque becomes

$$T_e = \frac{3}{2}\frac{P}{2}\frac{L_m^2}{L_r}\frac{i^e_{ds}}{1+\tau_r p} i^e_{qs} \quad \text{where } \tau_r = \frac{L_r}{r_r} \qquad (3)$$

The electromagnetic torque is a product of the d–axis component of rotor flux (λ^e_{dr}) and q–axis component of stator current (i^e_{qs}). The flux λ^e_{dr} is governed by the d–axis component of the stator current (i^e_{ds}) and the governing equation is of first order. Hence if i^e_{ds} is kept constant, the torque can be independently controlled simply by adjusting the current i^e_{qs}. Thus the control action is very simple; one needs only to control d– and q–axes components of the stator current for an independent control of rotor flux and torque respectively. This concept is illustrated in Figure 1. Equations for transforming the current from stator to rotor flux frame of reference are:

$$i^e_{qs} = i_{qds}\sin\phi_r \qquad (4)$$
$$i^e_{ds} = i_{qds}\cos\phi_r \qquad (5)$$

Thus, it is obvious that for the desired decoupling, updated knowledge of the value of the rotor flux angle ϕ_r is required.

III. Review Of Flux Tracking Methods

To date, realization of direct field orientation without a position sensor has, for the most part, been largely restricted to operation above 2-5 Hz because of practical problems associated at near standstill frequencies [2]. However, attempts have been made recently to overcome this barrier by monitoring second order non-linear flux related effects in the machine [8]-[10]. In general, these methods resort to using a high frequency test signal injection which is employed to extract information about the air gap / stator / rotor flux in the machine under test. The machine operation, however, remains governed by flux and torque components of the fundamental current that is superimposed on this test signal.

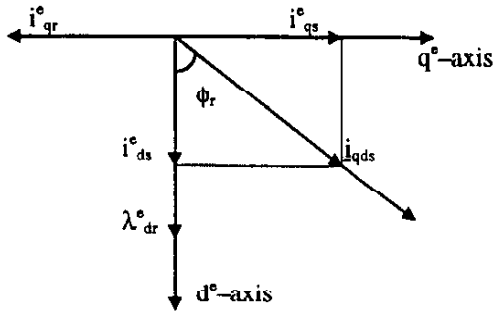

Figure 1. Vector diagram for rotor flux oriented induction machine model.

Blaschke et al. have proposed high frequency current injection to detect the variation of magnetizing reactances in the d– and q–axes [8]. This technique is based on the premise that since the flux in the machine is predominantly in d–axis, the magnetizing reactance in that axis is smaller than that in the q–axis owing to saturation as shown in Figure 2.

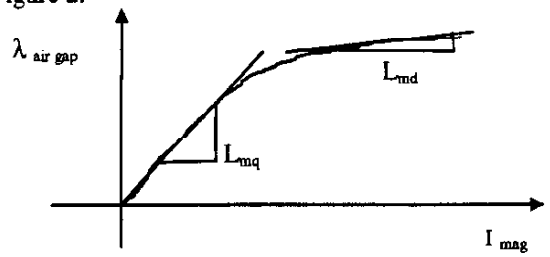

Figure 2. Magnetizing reactances in d– and q–axes.

For high frequency (ω_h) stator currents, one can approximately write the relations between stator and rotor currents in a synchronous (rotating at ω_h) frame of reference as

$$i^h_{dr} = -\frac{1}{1+L_{lr}/L_{md}}\, i^h_{ds} \qquad (6)$$

$$i^h_{qr} = -\frac{1}{1+L_{lr}/L_{mq}}\, i^h_{qs} \qquad (7)$$

Since the magnetizing reactances in d– and q–axes are not equal, scaling ratios between stator and rotor currents in these axes as given by equations (6) and (7) are different. This implies that a high frequency current injection ($\Delta \underline{i}_s$) in an improper d–axis will result in a displacement (γ) in the corresponding rotor current ($\Delta \underline{i}_r$). This effect is illustrated in Figure 3.

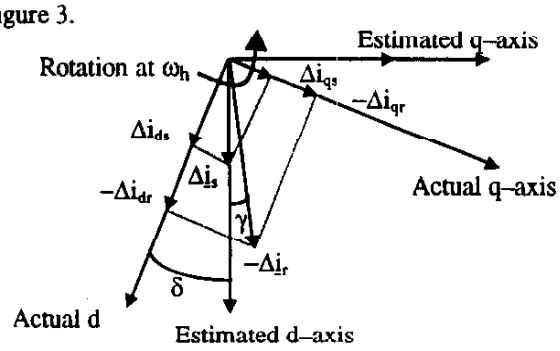

Figure 3. High frequency current injection in a *wrong* d-axis produces a displacement in the corresponding rotor current.

The displacement angle γ is proportional to the error angle δ between the estimated and actual flux axis and can thus be used directly to rectify errors in the flux angle estimation. However, this approach will, as stated, require knowledge of the rotor currents. Instead, the authors have presented an alternative strategy. One can write an approximate voltage equation in the test signal synchronous (rotating at ω_h) frame of reference as follows,

$$\Delta \underline{v}^h_s = \Delta \underline{i}^h_s r_s - \Delta \underline{i}^h_r r_r + \frac{d}{dt}\Delta \underline{i}^h_s L_{ls} - \frac{d}{dt}\Delta \underline{i}^h_r L_{lr} \qquad (8)$$

Similarly, in a mirror image of the test signal synchronous frame of reference about estimated d–axis, the voltage equation is

$$\Delta \underline{v}^h_{s-} = \Delta \underline{i}^h_s r_s - \Delta \underline{i}^h_r r_r - \frac{d}{dt}\Delta \underline{i}^h_s L_{ls} + \frac{d}{dt}\Delta \underline{i}^h_r L_{lr} \qquad (9)$$

Adding equations (8) and (9),

$$\Delta \underline{v}^h_s + \Delta \underline{v}^h_{s-} = 2\,\Delta \underline{i}^h_s r_s - 2\,\Delta \underline{i}^h_r r_r \qquad (10)$$

As is evident, the quadrature component of the left-hand side of equation (10) directly gives information concerning the displacement angle γ.

Although theoretically very attractive, this method is clearly computation intensive as well. Hence the method poses significant problems in practical implementation.

An alternative method has been reported which is based on the difference in the machine impedances in d– and q–axes [9]. For low frequency (ω_e) stator excitation, one can approximately write the circuit equations for d– and q–axes in a synchronous (rotating at ω_e) frame of reference as

$$v^e_{ds} = \left(r_s + p\,\sigma L_s + p\,\frac{r_r L_m^2}{L_r (r_r + pL_r)} \right) i^e_{ds} \qquad (11)$$

$$v^e_{qs} = (r_s + p\,\sigma L_s)\, i^e_{qs} \qquad (12)$$

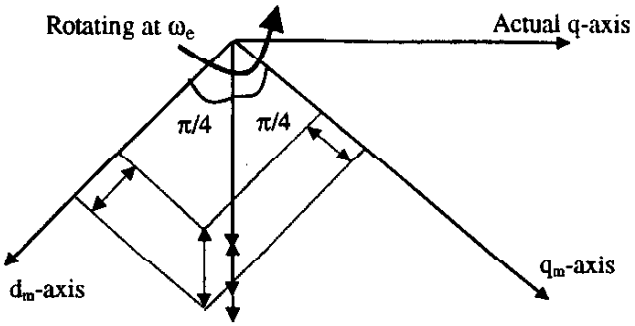

Figure 4. High frequency test signal in the *correct* d–axis produces an equal perturbation in the monitoring axes.

If a high frequency test signal is superimposed in the d–axis circuit, skin effect in the rotor resistance becomes more prominent, thereby causing a difference in equivalent d– and q–axis impedances. This difference can be detected by monitoring the corresponding perturbations in the d_m and q_m axes which are placed at 45° on either side of the estimated d–axis (Figures 4 and 5).

If the estimated d–axis is accurate then the resulting perturbations in the monitoring axes caused by high frequency injection are of equal amplitude (Figure 4); whereas if the estimated d–axis is incorrect, then the test signal can be resolved into the actual d– and q–axis components. This produces the corresponding unequal perturbations in the monitoring axes as shown in Figure 5.

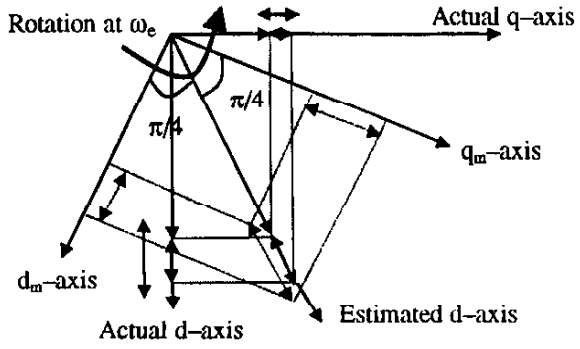

Figure 5. High frequency test signal in the *wrong* d–axis produces an unequal perturbation in the monitoring axes.

The authors of this paper have presented several methods to implement this scheme; viz. voltage injection and current injection. In the voltage injection scheme, corresponding currents are monitored, while in the current injection scheme corresponding voltages are monitored. It is shown that the error in estimation of flux angle is approximately proportional to the difference in the squares of voltages / currents in monitored axes in current / voltage injection systems.

Both the above methods, one depending upon variation in magnetizing reactance and the second depending on variation in rotor resistance, use the high frequency test signal injection in the d–axis only. This approach does not generate any torque ripple and causes less audible noise. However, the saliency image tracking can be enhanced by employing a rotating test signal in the machine under test instead of fluctuating signal injection. Jansen et al [10] have reported an approach to track the saliency in the stator transient reactance with three-phase balanced test excitation. The saturation induced saliency in the stator transient reactance in synchronous (rotating at ω_e) frame of reference is represented by

$$\sigma L^e_s = \begin{bmatrix} \sigma L_{qs} & 0 \\ 0 & \sigma L_{ds} \end{bmatrix} \qquad (13)$$

In the stationary frame of reference, this inductance becomes

$$\sigma L^s_s = \begin{bmatrix} \sigma L_{so} + \Delta\sigma L_s \cos 2\omega_e t & -\Delta\sigma L_s \sin 2\omega_e t \\ -\Delta\sigma L_s \sin 2\omega_e t & \sigma L_{so} - \Delta\sigma L_s \cos 2\omega_e t \end{bmatrix} \qquad (14)$$

where $\sigma L_{so} = \dfrac{\sigma L_{qs} + \sigma L_{ds}}{2}$ $\qquad \Delta\sigma L_s = \dfrac{\sigma L_{qs} - \sigma L_{ds}}{2}$

Therefore, if a balanced three-phase high frequency voltage is applied as follows

$$V^s_s = \begin{bmatrix} V_s \cos \omega_h t \\ -V_s \sin \omega_h t \end{bmatrix} \qquad (15)$$

the stator currents will be induced of the form

$$I^s_s = \begin{bmatrix} I_1 \sin \omega_h t + I_2 \sin (2\omega_e t - \omega_h t) \\ I_1 \cos \omega_h t + I_2 \cos (2\omega_e t - \omega_h t) \end{bmatrix} \qquad (16)$$

The second term in both the q– and d–axes has useful information about the position of flux. This can be extracted using demodulation and closed loop tracking filter.

A fundamental problem associated with all these methods is that they rely on the parameter tracking in d–q domain. This paper focuses on utilizing the actual phase information, rather than utilize d–q domain, to locate the flux in the machine under test. Not only is this approach intuitively more convincing, but also it has been observed that the variation in phase impedance directly determines the flux. The following section introduces the proposed flux tracking method based on phase impedance variation.

IV. Flux Tracking Method Based On Phase Impedance Variation

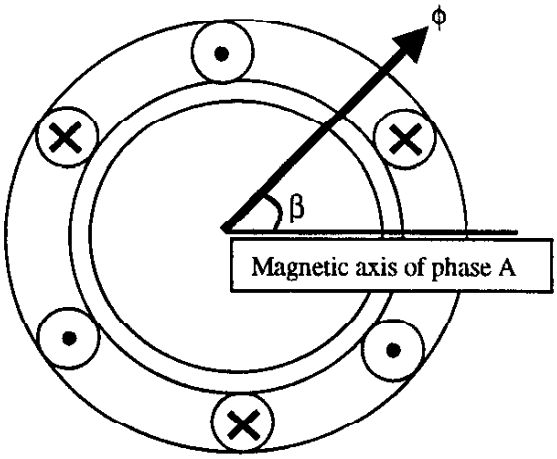

Figure 6. Rotating flux vector produced by a three-phase balanced excitation in an induction machine.

It is well known that a rotating magnetic field of constant amplitude is produced in a three-phase induction machine when it is excited with a three-phase balanced sinusoidal supply. This is depicted in Figure 6. A set of balanced three-phase currents of amplitude I_s and with angular frequency (ω_e) is given as

$$i_a = I_s \cos \omega_e t$$
$$i_b = I_s \cos (\omega_e t - 120^o)$$
$$i_c = I_s \cos (\omega_e t + 120^o) \quad (17)$$

the resultant mmf is given by

$$F = F_m \cos (\omega_e t - \beta) \quad (18)$$

It may be easily verified from the above equations that mmf in the magnetic axis of any particular phase is maximum when the current in that phase is maximum.

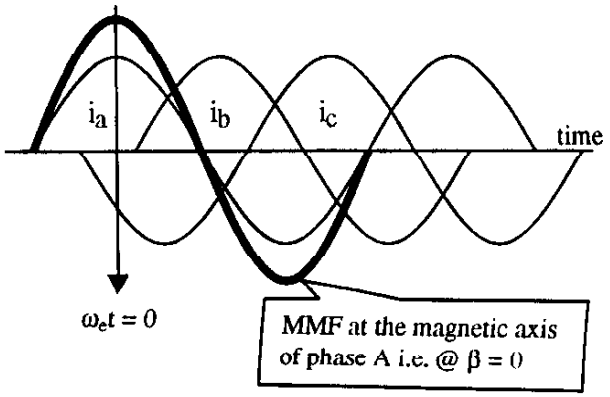

Figure 7. Time relation between phase currents and mmf at magnetic axis of phase A.

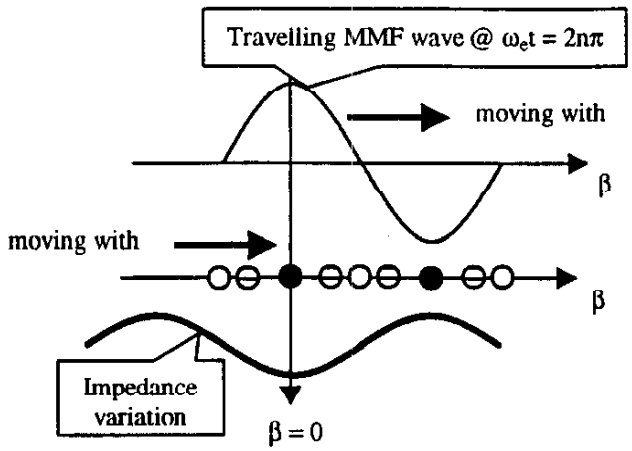

Figure 8. Spatial relation between phase A impedance and mmf at magnetic axis of that phase.

An example case for phase A is shown in Figure 7. As may be seen from this figure, the mmf at the magnetic axis of phase A (heavy line) follows the current in that phase (i_a). Consider further a special case when the mmf is a maximum at $\beta = 0$ as shown in Figure 8. We assume here a normal machine with a squirrel cage with embedded rotor slots. Under the condition of Figure 8, the rotor bars at spatial positions $\beta = -\pi/2$ and $\beta = \pi/2$ have a very small flux associated with them and hence, they come out of saturation. Consequently these bars offer a higher reactance than the bars at $\beta = 0$ and $\beta = \pi$ which encounter maximum flux and are saturated. This effect causes a saliency in the individual phase impedance. Hence, if the impedance of each phase is monitored, one can detect this saturation-induced saliency and consequently track the rotating flux vector. This is the central theme of the proposed method of this paper.

It may be noted that the impedance of a phase is minimum when the flux (air gap flux density) associated with it is maximum. Figure 9 illustrates the relationship between the location of the flux in the machine, individual phase impedance and the phase A current under a no-load condition. It should be noted that the spatial angle β is calculated from the magnetic axis of phase A. For a loaded condition, the flux vector lags the current vector. This lag angle is load dependent. As the variation in individual phase impedance is strictly a function of flux location and the machine structure, it will also lag the current like the flux. However the relation between the flux location and phase impedance is invariant. Thus, irrespective of the load and speed conditions, the impedance variation will always be locked to the flux vector.

It is interesting to note the relative behavior of phase A current and impedance in the same phase. When this current

is at its peak, the stator produced flux in the magnetic axis of phase A is maximum. This causes saturation of the corresponding rotor bars which consequently decreases the impedance. On the other hand, when the current is zero, the rotor bars come out of saturation thereby increasing the effective impedance.

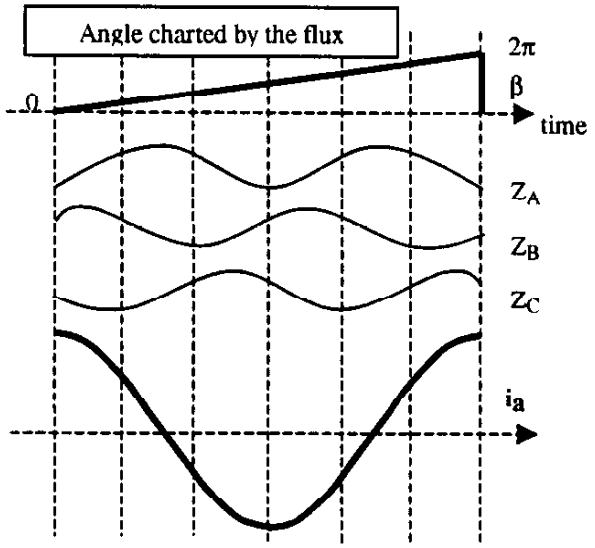

Figure 9. Relation between the location of the flux vector, individual phase impedance and phase A current in the no-load condition.

V. Techniques To Detect Phase Impedance Variation And Their Practical Implementation

As explained in the earlier section, a saliency is caused in the phase impedance owing to the rotor bar saturation effects. If the impedance associated with each phase is monitored, one can detect this saturation-induced saliency and consequently track the rotating flux vector. A simple method to do this would be to inject a test signal in each phase and monitor the impedance associated with it by measuring the corresponding phase voltages. With this approach, one would obtain the phase impedance variation with twice the frequency of fundamental excitation as depicted in Figure 9. It is important to note that the nominal value of phase impedance and the actual magnitude of variation depends on various machine parameters but is insignificant in determining the location of flux. As the rotating flux in the machine causes variation in the phase impedance, tracking these alternate maxima and minima will directly lead to determining of flux. Hence, first the offsets in individual phase impedances are nullified and their values are normalized. This produces a set of three balanced sinusoidal waveforms with their peaks signifying the maximum and minimum flux occurrences. Next when one applies a d–q transformation on these waveforms a cosine and a sine waveform is generated. It may be noted that mere application of the d–q transformation on the normalized phase impedances does not transform them into equivalent d–q impedances. The resultant quantities do not have great physical significance and the d–q transformation is simply utilized as a means to obtain the sine and cosine waveforms. Finally, the flux angle is extracted by a demodulation procedure as shown in Figure 10.

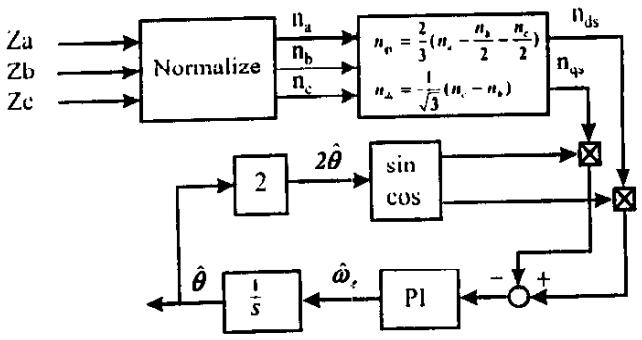

Figure 10. Block schematic of the procedure for flux angle extraction from individual phase reactances.

The three-phase balanced test current, by itself, will produce rotating flux, thereby interfering with the nominal machine operation and this interference must be minimized. There are two alternatives to realize an unbalanced high frequency signal injection as shown in Figures 11 and 12. The first method to inject a test current in only two phases (Figure 11). For such test signals, one phase of the machine is effectively "Open". These test currents with amplitude I_h and frequency ω_h are given as follows :

$$I_{an} = 0$$
$$I_{bn} = -I_h \sin\omega_h t$$
$$I_{cn} = I_h \sin\omega_h t \qquad (19)$$

It may be noted that above expressions for phase currents are valid only for the test signals. These test signals are superimposed on the fundamental components required for flux and torque.

An alternative method to inject an unbalanced current is as shown in Figure 12. The test currents in B and C phases are controlled to be identical so that they emulate a phase to phase short circuit condition. The expressions for test currents are given as follows :

$$I_{an} = I_h \sin\omega_h t$$
$$I_{bn} = -0.5\, I_h \sin\omega_h t$$
$$I_{cn} = -0.5\, I_h \sin\omega_h t \qquad (20)$$

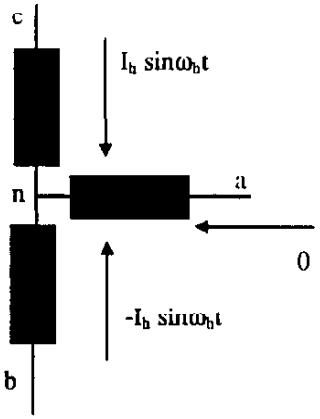

Figure 11. Single phase high frequency test current with phase A open.

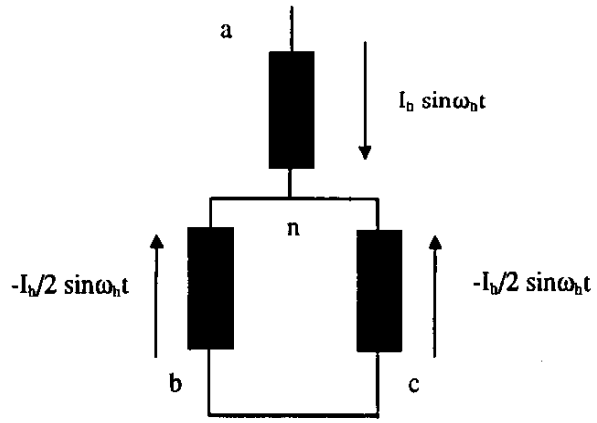

Figure 12. Single phase high frequency test current with phases B and C shorted.

VI. Experimental Results

A 10 hp general purpose induction machine was employed to test the feasibility of the proposed tracking methodology. The machine characteristics are presented in the appendix. A three-phase balanced excitation is employed to track phase impedance variation in order to locate the flux in the machine under test. The machine is controlled by an indirect field oriented controller and is operated at 0.3 Hz at no load. Figures 13 and 14 show actual and normalized phase impedances respectively obtained with the high frequency test injection technique.

As may be seen from Figure 14, the normalized phase impedances are a set of three balanced waveforms with twice the excitation frequency. Next a d–q transformation is applied on these impedances which results in a sine and a cosine waveform. These are presented in Figures 15 and 16 for forward and reverse direction of rotation. Finally, the flux angle is determined by demodulation. The result of estimation, especially when the machine is reversing the direction, is presented in Figure 17. It shows the estimated flux angle, phase A current, actual stator frequency and estimated stator frequency.

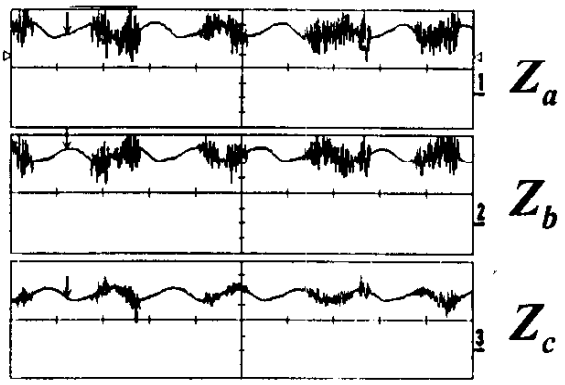

Figure 13. Three-phase impedances of the machine under test.

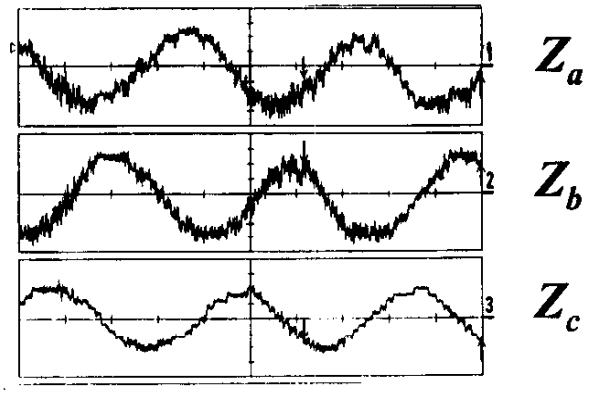

Figure 14. Normalized phase impedances of the machine under test.

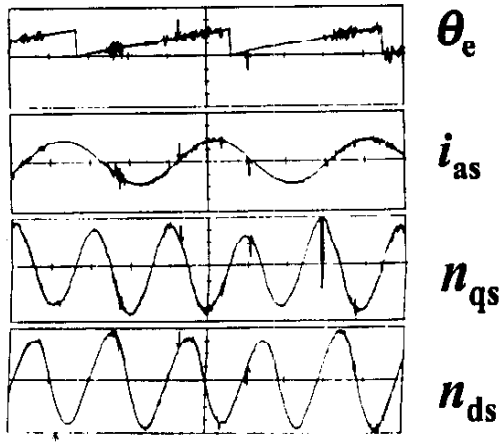

Figure 15. d–q transformed impedances (forward mode).

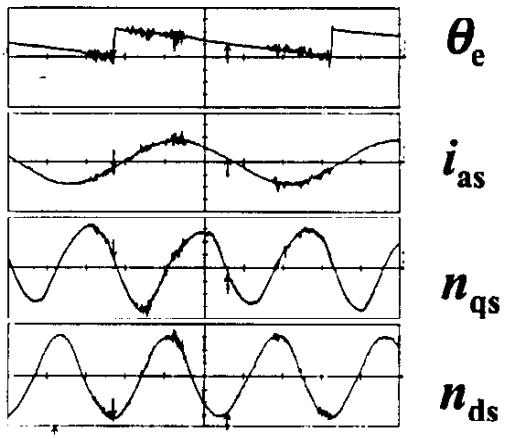

Figure 16. d–q transformed impedances (reverse mode).

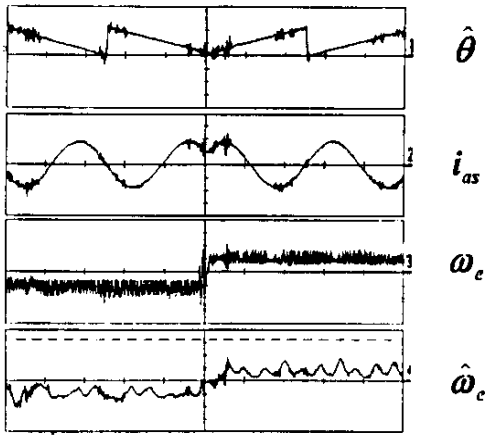

Figure 17. Flux estimation during direction reversal.

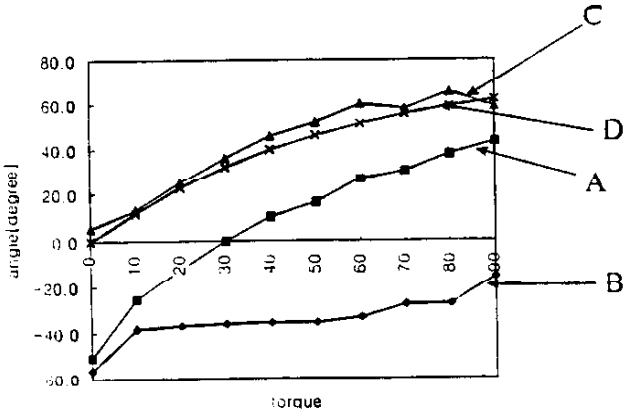

Figure 18. Relation between the actual rotor flux angle and the estimated flux angle over the range of torque control.

Figure 18 shows the rotor flux angle obtained from the indirect field oriented controller (Trace D) over the entire range of torque control. Trace A in the same figure shows the estimated flux obtained by the proposed technique over this range. By using a small correction factor (Trace B), it is possible to predict the rotor flux with good accuracy (Trace C) in order to be capable of independent torque control. However this correction factor is machine and operating point dependent and hence not recommended. Further work involves adding an on-line controller to eliminate the correction factor and will be reported in the future.

VII. Conclusions

A summary of the state-of-the-art in machine flux determination by injecting high frequency signals is presented. A novel technique based on similar high frequency injection is described. It is demonstrated that the rotating flux vector in the machine causes saturation-induced saliency in the phases under normal operating conditions. By employing high frequency test signals, this saliency is monitored which is then used to track the flux in the machine. The experimental results confirm the feasibility and efficacy of the proposed tracking approach.

These flux tracking methods can be employed to accomplish direct field orientation for torque control purposes. However, it is important to note that, in testing this flux tracking performance, the machine under test was governed by a different (indirect field oriented) controller. The experimental results presented in this paper only confirm the claim of phase impedance variation and its association with the flux in the machine under test. It is observed that, irrespective of the load and speed conditions, the impedance variation is always locked to some flux angle so that the signal can be used as a feedback signal to achieved field oriented control.

References

[1] F. Blaschke, "*Das Verfahren der Feldorientierung zur Regelung der Drehfeldmaschine*," Ph. D. thesis, TU Braunschweig, 1974.

[2] T.A. Lipo and D.W. Novotny, "*Vector Control and Dynamics of AC Drives*," Oxford, 1996.

[3] D. Zinger, F. Profumo, T.A. Lipo, D.W. Novotny, "A direct field oriented controller for induction machines using tapped stator windings," *Conference Record of the IEEE-PESC*, 1988, pp. 855-861.

[4] X. Xu, R.W. DeDoncker, D.W. Novotny, "A stator flux oriented induction machine drive," *Conference Record of the IEEE-PESC*, 1988, pp. 870-876.

[5] J.C. Moreira, T.A. Lipo, "A new method for rotor time constant tuning in indirect field oriented control", *Conference Record of the IEEE-PESC*, 1990, pp. 573-580.

[6] V. Blasko, T. Matsuo, J.C. Moreira, T.A. Lipo, "A new direct field oriented controller employing rotor end ring

current detection", *Conference Record of the IEEE-PESC*, 1990, pp. 599-605.

[7] M. Schroedl, "Sensorless control of ac machines at low speeds and standstill based on the INFORM method," *Conference Record of the IEEE-IAS Annual Meeting*, 1996, pp. 270-277.

[8] F. Blaschke, J. van der Burgt, A. Vandenput, "Sensorless direct field orientation at zero flux frequency," *Conference Record of the IEEE-IAS Annual Meeting*, 1996, pp. 189-196.

[9] J.I. Ha and S.K. Sul, "Sensorless field orientation control of an induction machine by high frequency signal injection," *Conference Record of the IEEE-IAS Annual Meeting*, 1997, pp. 426-432.

[10] P.L. Jansen and R.D. Lorenz "Transducerless field orientation concepts employing saturation-induced saliencies in induction machines," *IEEE Transactions on I.A.*, Vol. IA-32, No. 6, Nov/Dec 1996, pp. 1380-1393.

APPENDIX

Name plate data of machine under test

Manufacturer	Baldor Inc.
Rated Power	10 Horse Power
Rated Voltage	230 V
Number of Phases	3
Number of Poles	4
Rated Frequency	60 Hz
Type of Rotor and Rotor Slot	Squirrel cage / Closed Slot